arXiv:1105.2284v2 [hep-ph] 18 Nov 2011

CERN-PH-TH/2011-106
DESY 11-075

Higgs Portal Inflation

Oleg Lebedev [a] **and Hyun Min Lee** [b]

a: *DESY Theory Group, Notkestrasse 85, D-22607 Hamburg, Germany*

b: *CERN, Theory Division, CH-1211 Geneva 23, Switzerland*

Abstract

The Higgs sector of the Standard Model offers a unique opportunity to probe the hidden sector. The Higgs squared operator is the only dimension two operator which is Lorentz and gauge invariant. It can therefore couple both to scalar curvature and the hidden sector at the dim–4 level. We consider the possibility that a combination of the Higgs and a singlet from the hidden sector plays the role of inflaton, due to their large couplings to gravity. This implies that the quartic couplings satisfy certain constraints which leads to distinct low energy phenomenology, including Higgs signals at the LHC. We also address the unitarity issues and show that our analysis survives the unitarization procedure.

1 Introduction

Cosmic inflation [1] is a paradigm beyond the Standard Big Bang Cosmology which addresses the flatness, isotropy, homogeneity, horizon and relic problems. Furthermore, quantum fluctuations during inflation provide a seed for the large–scale structure formation. On the other hand, the nature of the inflaton remains a mystery. It has recently been conjectured that the only scalar of the Standard Model (SM), the Higgs field, may play its role [2], given a large Higgs coupling to scalar curvature. The Higgs sector is also quite special because it has a direct access to the "hidden sector" [3], whose existence is motivated by various ideas including string theory, dark matter, etc. Understanding the Higgs couplings would thus provide us with unique information about the hidden world.

There are two dim-2 operators in the Standard Model that can couple to the hidden sector at the renormalizable level: $F^Y_{\mu\nu}$ and $H^\dagger H$. The latter is also Lorentz invariant, so it can in addition couple to scalar curvature R. One can therefore add the following dim–4 operators to the Standard Model Lagrangian,

$$\begin{aligned} \Delta\mathcal{L}_1 &= c_1\ H^\dagger H|S|^2\ , \\ \Delta\mathcal{L}_2 &= c_2\ H^\dagger H R\ , \end{aligned} \tag{1}$$

where S is a singlet under the Standard Model and c_i are dimensionless constants. In what follows, we consider the minimal option for the hidden sector: we take S to be a real scalar s and impose the symmetry $s \leftrightarrow -s$. The coupling c_1 controls the Higgs decay into the hidden sector as well as the Higgs–singlet mixing, which can be measured at the LHC. c_2 can be responsible for inflation: with $|c_2| \gg 1$, a large value of the Higgs field in the early universe leads to exponential expansion.

In this work, we consider the possibility that the inflaton is a mixture of the Higgs with the singlet from the hidden sector. The nature of the inflaton depends on the relations among various couplings. For example, if c_1 is positive, stability of the potential requires a mixed inflaton. On the other hand, for negative c_1 the inflaton can be purely the Higgs or the singlet field. These considerations leave an imprint on the low energy physics, affecting the couplings of the Higgs–like particles to be studied at the LHC.

We also study the unitarity issues which plague the original Higgs inflation [4, 5]. We construct a unitary completion [6] of the Higgs portal inflation and show that the constraints on the couplings survive the unitarization procedure.

The paper is organized as follows. We first present a general analysis of the SM extension with a real singlet in the presence of large couplings to scalar curvature. We study stability of the system during inflation and derive the corresponding constraints on the couplings. Then we study implications for low energy physics. We further discuss the differences from the pure Higgs [7] and singlet inflation [8, 9], and present an example of the unitary completion of our model.

2 Higgs–singlet combination as the inflaton

In this section, we study an extension of the Higgs sector with a real scalar s in the presence of large couplings $\xi_{h,s}$ to scalar curvature R. This system can lead to inflation based on scale invariance of the Einstein frame scalar potential at large field values. The relevant Jordan frame Lagrangian in the unitary gauge $H^T = (0, h/\sqrt{2})$ is

$$\mathcal{L}/\sqrt{-g} = -\frac{1}{2}M_{\rm Pl}^2 R - \frac{1}{2}\xi_h h^2 R - \frac{1}{2}\xi_s s^2 R + \frac{1}{2}(\partial_\mu h)^2 + \frac{1}{2}(\partial_\mu s)^2 - V \tag{2}$$

with $\xi_{h,s} > 0$[1] and

$$V = \frac{1}{4}\lambda_h h^4 + \frac{1}{4}\lambda_{hs} s^2 h^2 + \frac{1}{4}\lambda_s s^4 + \frac{1}{2}m_h^2 h^2 + \frac{1}{2}m_s^2 s^2 \ . \tag{3}$$

The transformation to the Einstein frame, in which the only coupling to curvature is $-1/2M_{\rm Pl}^2 R$, is defined by

$$\tilde{g}_{\mu\nu} = \Omega^2 g_{\mu\nu} \quad , \quad \Omega^2 = 1 + \frac{\xi_h h^2 + \xi_s s^2}{M_{\rm Pl}^2} \ . \tag{4}$$

Consider now the limit

$$\xi_h h^2 + \xi_s s^2 \gg M_{\rm Pl}^2 \tag{5}$$

and set $M_{\rm Pl}$ to 1. In this case, $\Omega^2 \simeq \xi_h h^2 + \xi_s s^2$. Then, according to [10], the kinetic terms and the potential in the Einstein frame take the form

$$\begin{aligned} \mathcal{L}_{\rm kin} &= \frac{3}{4}\left(\partial_\mu \log(\xi_h h^2 + \xi_s s^2)\right)^2 + \frac{1}{2}\frac{1}{\xi_h h^2 + \xi_s s^2}\left((\partial_\mu h)^2 + (\partial_\mu s)^2\right) , \\ U &= \frac{1}{(\xi_h h^2 + \xi_s s^2)^2}\ V \ . \end{aligned} \tag{6}$$

Introduce new variables

$$\begin{aligned} \chi &= \sqrt{\frac{3}{2}}\ \log(\xi_h h^2 + \xi_s s^2) \ , \\ \tau &= \frac{h}{s} \ . \end{aligned} \tag{7}$$

[1] We do not consider negative ξ_i since in this case the theory is not well defined at large field values.

In terms of these variables, the kinetic terms read

$$\begin{aligned}\mathcal{L}_{\rm kin} &= \frac{1}{2}\left(1+\frac{1}{6}\frac{\tau^2+1}{\xi_h\tau^2+\xi_s}\right)(\partial_\mu\chi)^2+\frac{1}{\sqrt{6}}\,\frac{(\xi_s-\xi_h)\tau}{(\xi_h\tau^2+\xi_s)^2}(\partial_\mu\chi)(\partial^\mu\tau)\\ &+ \frac{1}{2}\frac{\xi_h^2\tau^2+\xi_s^2}{(\xi_h\tau^2+\xi_s)^3}(\partial_\mu\tau)^2\ .\end{aligned} \tag{8}$$

We are interested in the case of large non-minimal couplings, $\xi\equiv\xi_h+\xi_s\gg 1$. Since the $(\partial_\mu\tau)^2$ term scales like $1/\xi$ and so does the mixing term $(\partial_\mu\chi)(\partial^\mu\tau)$, in terms of (approximately) canonically normalized variables the mixing is suppressed. Then, to leading order in $1/\xi$, we have

$$\mathcal{L}_{\rm kin}=\frac{1}{2}(\partial_\mu\chi)^2+\frac{1}{2}\frac{\xi_h^2\tau^2+\xi_s^2}{(\xi_h\tau^2+\xi_s)^3}(\partial_\mu\tau)^2\ . \tag{9}$$

In the following limiting cases, one can define a particularly simple canonically normalized variable τ' :

$$\begin{aligned}&\xi_s\gg\xi_h \ \text{ or } \ \tau\to 0\ , && \tau'=\frac{\tau}{\sqrt{\xi_s}}\ ,\\ &\xi_h\gg\xi_s \ \text{ or } \ \tau\to\infty\ , && \tau'=\frac{1}{\sqrt{\xi_h}\tau}\ ,\\ &\xi_h=\xi_s\ , && \tau'=\frac{1}{\sqrt{\xi_h}}\arctan\tau\ .\end{aligned} \tag{10}$$

The scalar potential at large χ reads

$$U=\frac{\lambda_h\tau^4+\lambda_{hs}\tau^2+\lambda_s}{4(\xi_h\tau^2+\xi_s)^2}\ . \tag{11}$$

Its minima are classified according to

$$\begin{aligned}&(1)\ 2\lambda_h\xi_s-\lambda_{hs}\xi_h>0\ ,\ 2\lambda_s\xi_h-\lambda_{hs}\xi_s>0\ , && \tau=\sqrt{\frac{2\lambda_s\xi_h-\lambda_{hs}\xi_s}{2\lambda_h\xi_s-\lambda_{hs}\xi_h}}\ ,\\ &(2)\ 2\lambda_h\xi_s-\lambda_{hs}\xi_h>0\ ,\ 2\lambda_s\xi_h-\lambda_{hs}\xi_s<0\ , && \tau=0\ ,\\ &(3)\ 2\lambda_h\xi_s-\lambda_{hs}\xi_h<0\ ,\ 2\lambda_s\xi_h-\lambda_{hs}\xi_s>0\ , && \tau=\infty\ ,\\ &(4)\ 2\lambda_h\xi_s-\lambda_{hs}\xi_h<0\ ,\ 2\lambda_s\xi_h-\lambda_{hs}\xi_s<0\ , && \tau=0,\infty\ .\end{aligned} \tag{12}$$

Note that in the last case there are 2 local minima. We are primarily interested in the first case, when the inflaton is a combination of the Higgs field and the singlet. The corresponding value of the potential is then

$$U\Big|_{\rm min\ (1)}=\frac{1}{16}\frac{4\lambda_s\lambda_h-\lambda_{hs}^2}{\lambda_s\xi_h^2+\lambda_h\xi_s^2-\lambda_{hs}\xi_s\xi_h}\ , \tag{13}$$

while in cases (2) and (3), it is $\lambda_s/(4\xi_s^2)$ and $\lambda_h/(4\xi_h^2)$, respectively. The condition $4\lambda_s\lambda_h-\lambda_{hs}^2>0$ guarantees the absence of very deep minima with negative vacuum energy at field values $m_{h,s}\ll$

h, s, which make the electroweak vacuum metastable. With this constraint, the vacuum energy above is positive (the denominator is positive by the minimization conditions).

In all of the cases, the τ-field is heavy and can be integrated out. Indeed, the mass of the canonically normalized τ' scales as $1/\sqrt{\xi}$ in Planck units, while the Hubble rate scales like $\sqrt{U}|_{\rm min} \sim 1/\xi$. Thus

$$m_{\tau'}^2 \gg H^2 \, . \tag{14}$$

The potential value (13) plays the role of the quartic coupling over ξ^2 in the single field inflation model of Bezrukov–Shaposhnikov [2]. Retaining the subleading $M_{\rm Pl}^2/(\xi_h h^2 + \xi_s s^2)$ term in Ω^2, the inflaton potential for option (1) becomes

$$U(\chi) = \frac{\lambda_{\rm eff}}{4\xi_h^2} \left(1 + \exp\left(-\frac{2\chi}{\sqrt{6}}\right)\right)^{-2} \tag{15}$$

in Planck units, where

$$\lambda_{\rm eff} = \frac{1}{4} \frac{4\lambda_s\lambda_h - \lambda_{hs}^2}{\lambda_s + \lambda_h x^2 - \lambda_{hs} x} \tag{16}$$

and

$$x = \frac{\xi_s}{\xi_h} \, . \tag{17}$$

The inflationary parameters are read off from this potential [2]. At large χ, the potential is flat and inflation takes place. As χ rolls to smaller values, the ϵ-parameter approaches 1 and inflation ends. In terms of

$$\tilde{h} \simeq \frac{1}{\sqrt{\xi_h}} \, \exp\bigl(\chi/\sqrt{6}\bigr) \, , \tag{18}$$

the ϵ-parameter is given by

$$\epsilon = \frac{1}{2}\left(\frac{dU/d\chi}{U}\right)^2 \simeq \frac{4}{3\xi_h^2 \tilde{h}^4} \, . \tag{19}$$

This gives $\tilde{h}_{\rm end} = (4/3)^{1/4}/\sqrt{\xi_h}$. Then, for a given number of e-folds N, the initial value of the inflaton is $\tilde{h}_{\rm in} \approx \sqrt{4N/(3\xi_h)}$. Together with the COBE normalization $U/\epsilon = 0.027^4$ [11], this fixes ξ_h in terms of $\lambda_{\rm eff}$,

$$\xi_h \simeq \sqrt{\frac{\lambda_{\rm eff}}{3}} \, \frac{N}{0.027^2} \, . \tag{20}$$

For $\sqrt{\lambda_{\rm eff}} \sim 1$ and $N = 60$, the non-minimal gravity coupling ξ_h is about 50000. The spectral index is predicted to be

$$n \simeq 1 - \frac{2}{N} \simeq 0.97 \, , \tag{21}$$

while the tensor to scalar perturbation ratio is $r \simeq 12/N^2 \simeq 0.0033$. These are robust (tree–level) predictions of our framework to be tested in the future.[2] They are independent of the

[2] In multi–field variants of this scenario, large non–Gaussianity can also be generated [12].

nature of the inflaton and result from the shape of the potential, which in turn follows from a large coupling to scalar curvature.

2.1 Parameter space analysis

In this subsection, we analyze the parameter space consistent with the inflaton being a mixture of the Higgs and singlet fields. The relavant inflation parameters are evaluated at a high energy scale μ. A particular choice of μ advocated in [13] is to take $\mu \sim m_t(\chi)$ which minimizes the effect of logarithms in the Coleman-Weinberg potential. In this case, $\mu \sim M_{\rm Pl}/\sqrt{\xi}$ for large χ. However, as we discuss in Sec. 5, the theory is only well defined up to the scale $M_{\rm Pl}/\xi$ at which unitarity violation appears. We thus expect new physics to set in at the unitarity scale $\mu_U \sim M_{\rm Pl}/\xi$ and take μ_U as the scale at which the input parameters are specified. We will assume that the new physics does not significantly affect the tree level relations of the previous section (see an example in Sec. 5), yet it is likely to affect the running of the relevant parameters above μ_U. For successful Higgs–singlet inflation, we impose at μ_U:

$$\begin{aligned} &2\lambda_h x - \lambda_{hs} > 0 \,, \\ &2\lambda_s \frac{1}{x} - \lambda_{hs} > 0 \,, \\ &4\lambda_s\lambda_h - \lambda_{hs}^2 > 0 \,. \end{aligned} \tag{22}$$

The third inequality provides an independent constraint for $\lambda_{hs} < 0$, while for positive λ_{hs} it follows from the first two. In addition we require perturbativity and stability at μ_U:

$$\begin{aligned} &|\lambda_i| < 1 \,, \\ &\lambda_{h,s} > 0 \,. \end{aligned} \tag{23}$$

Our (judicial) definition of the perturbative couplings is motivated by perturbativity at the Planck scale. We note that above $M_{\rm Pl}/\xi$, the running of λ_i slows down due to the suppression of the inflaton self-coupling or, equivalently, suppression of its propagator in the Jordan frame (see, e.g. [8]). Therefore, our procedure is expected to take into account the bulk of radiative corrections. Finally, given uncertainties from new physics above μ_U, the running of the parameters, e.g. the spectral index [13, 14, 15, 16], during inflation cannot be reliably calculated in our framework and we therefore omit it.

The renormalization group (RG) equations governing the evolution of couplings below μ_U

are given by [8]:

$$\begin{aligned}
16\pi^2\frac{d\lambda_h}{dt} &= 24\lambda_h^2 - 6y_t^4 + \frac{3}{8}\Big(2g^4 + (g^2+g'^2)^2\Big) \\
&+ (-9g^2 - 3g'^2 + 12y_t^2)\lambda_h + \frac{1}{2}\lambda_{hs}^2 \ , \\
16\pi^2\frac{d\lambda_{hs}}{dt} &= 4\lambda_{hs}^2 + 12\lambda_h\lambda_{hs} - \frac{3}{2}(3g^2+g'^2)\lambda_{hs} \\
&+ 6y_t^2\lambda_{hs} + 6\lambda_s\lambda_{hs} \ , \\
16\pi^2\frac{d\lambda_s}{dt} &= 2\lambda_{hs}^2 + 18\lambda_s^2 \ ,
\end{aligned} \tag{24}$$

where $t = \ln(\mu/m_t)$. The RG equations for the gauge and the top Yukawa couplings can be found in [13]. The low energy input values for these couplings are $g(m_t) = 0.64, g'(m_t) = 0.35, g_3(m_t) = 1.16$, while for the top Yukawa coupling we use its running value at m_t, $y_t(m_t) = 0.93$ [17]. For a given set of the low energy couplings at $t = 0$, we use the above RG equations to run them up to $t \approx 26$ and impose the constraints (22) and (23).

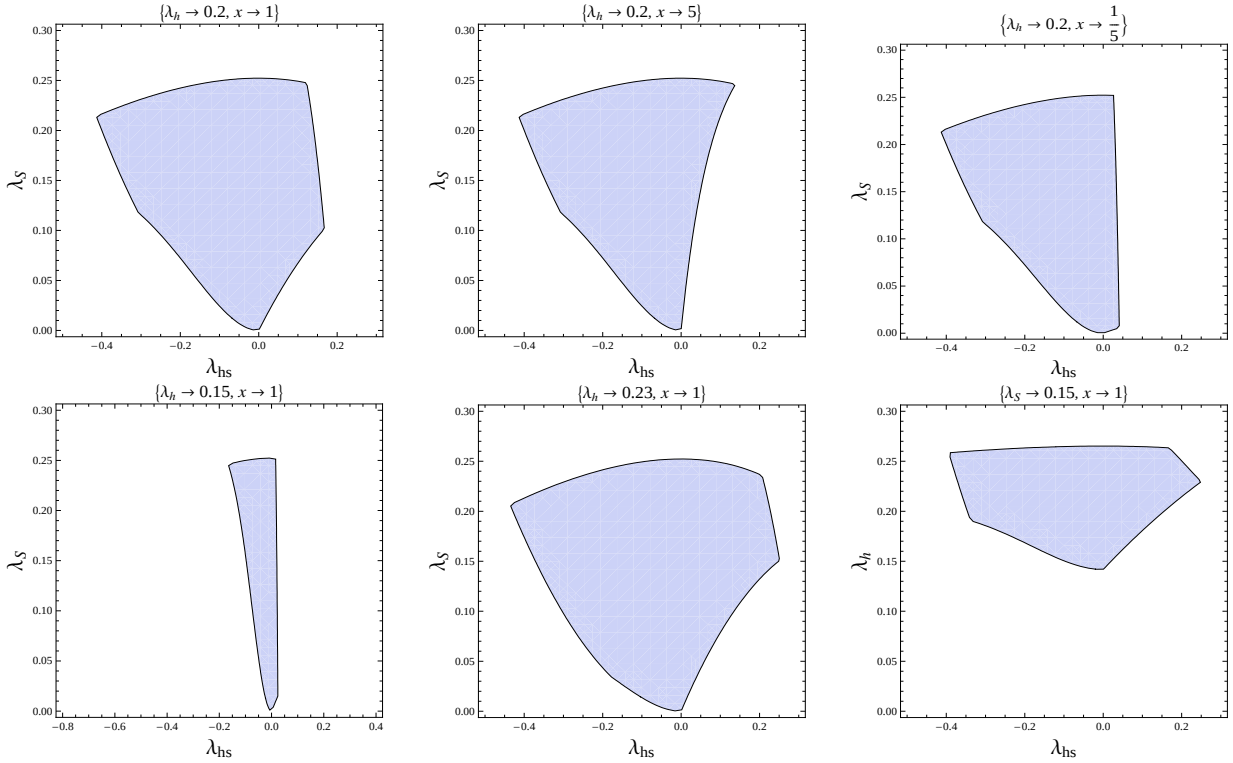


Figure 1: Parameter space consistent with the mixed Higgs–singlet inflaton. λ_i are given at the scale m_t, while x is a high energy input.

In addition, we impose the low energy constraint at m_t

$$4\lambda_s\lambda_h - \lambda_{hs}^2 > 0 \tag{25}$$

for $\lambda_{hs} < 0$. This ensures that there are no deep minima at some intermediate scale $s, h \gg m_s, m_h$ which can make the electroweak vacuum short-lived. It is a complementary constraint and (22) does not guarantee that it is satisfied. We find that for $\lambda_{hs} < 0$ the combination $\lambda_s\lambda_h$ can increase with energy faster than λ_{hs}^2 such that parameter space allowed by (22) may violate (25).

Our results are presented in Fig. 1. In the $\{\lambda_{hs}, \lambda_s\}$ plane, the parameter space at $\lambda_{hs} > 0$ is most strongly constrained by $2\lambda_s\frac{1}{x} - \lambda_{hs} > 0$ and, for larger λ_s, by $2\lambda_h x - \lambda_{hs} > 0$. In the latter case, λ_s contributes significantly to the running of λ_{hs}, but not to that of λ_h, which eliminates parameter space to the right of some critical value λ_{hs}. For negative λ_{hs}, the main constraint is $4\lambda_s\lambda_h - \lambda_{hs}^2 > 0$ (both at μ_U and m_t) as well as perturbativity which cuts off large values of λ_s and $|\lambda_{hs}|$. At $x \gg 1$ or $x \ll 1$, it becomes more difficult to satisfy either $2\lambda_s\frac{1}{x} - \lambda_{hs} > 0$ or $2\lambda_h x - \lambda_{hs} > 0$, so only small positive values of λ_{hs} are allowed. On the other hand, negative λ_{hs} are not affected by x. Decreasing λ_h eliminates most of the parameter space and leaves a strip around $\lambda_{hs} = 0$. The negative top quark contribution to the β–function of λ_h makes it run slower, reducing $\lambda_h(\mu_U)$ and making it more difficult to satisfy the constraints at μ_U. Naturally, at larger λ_h, parameter space opens up. The range of allowed λ_h is similar to that of the Standard Model subject to the perturbativity and stability requirements, i.e. roughly $0.14 < \lambda_h < 0.25$.

Note that the value of ξ_h is not important for our analysis. Given λ_{eff}, it is fixed at the scale μ_U by Eq.(20). Since we are not interested in its value at low energies, its running is not relevant for us.

3 Phenomenological implications

There are two phenomenologically acceptable possibilities for the vacuum of our theory: (a) $\langle h\rangle \neq 0, \langle s\rangle \neq 0$ and (b) $\langle h\rangle \neq 0, \langle s\rangle = 0$. They lead to different phenomenological implications.

3.1 $\langle h\rangle \neq 0, \langle s\rangle \neq 0$

Denoting $\langle h\rangle = v, \langle s\rangle = u$, extremization of the low energy scalar potential (3) requires

$$\begin{aligned} v^2 &= 2\ \frac{\lambda_{hs} m_s^2 - 2\lambda_s m_h^2}{4\lambda_s\lambda_h - \lambda_{hs}^2}\ , \\ u^2 &= 2\ \frac{\lambda_{hs} m_h^2 - 2\lambda_h m_s^2}{4\lambda_s\lambda_h - \lambda_{hs}^2}\ . \end{aligned} \tag{26}$$

The diagonal matrix elements of the Hessian at this point are $2\lambda_s u^2$ and $2\lambda_h v^2$, while its determinant is $(4\lambda_s\lambda_h - \lambda_{hs}^2)v^2u^2$. Then, the extremum is a local minimum if

$$\begin{aligned} &\lambda_{hs} m_h^2 - 2\lambda_h m_s^2 > 0\ , \\ &\lambda_{hs} m_s^2 - 2\lambda_s m_h^2 > 0\ , \\ &4\lambda_s\lambda_h - \lambda_{hs}^2 > 0\ . \end{aligned} \tag{27}$$

In this case, the mass squared eigenvalues are

$$m_{1,2}^2 = \lambda_h v^2 + \lambda_s u^2 \mp \sqrt{(\lambda_s u^2 - \lambda_h v^2)^2 + \lambda_{hs}^2 u^2 v^2} \tag{28}$$

with the mixing angle θ given by

$$\tan 2\theta = \frac{\lambda_{hs} uv}{\lambda_h v^2 - \lambda_s u^2}\ . \tag{29}$$

Here the mixing angle is defined by

$$O^T\ M^2\ O = \mathrm{diag}(m_1^2, m_2^2)\ \ ,\ \ O = \begin{pmatrix} \cos\theta & \sin\theta \\ -\sin\theta & \cos\theta \end{pmatrix}\ , \tag{30}$$

where M^2 is a 2×2 mass squared matrix. The range of θ is related to the ordering of the eigenvalues through $\mathrm{sign}(m_1^2 - m_2^2) = \mathrm{sign}(\lambda_s u^2 - \lambda_h v^2)\ \mathrm{sign}(\cos 2\theta)$ and we take m_1 to be the smaller eigenvalue. The mass eigenstates are

$$\begin{aligned} H_1 &= s\cos\theta - h\sin\theta\ , \\ H_2 &= s\sin\theta + h\cos\theta\ . \end{aligned} \tag{31}$$

Note that the lighter mass eigenstate H_1 is "Higgs–like" for $\lambda_s u^2 > \lambda_h v^2$ and "singlet–like" otherwise. The former case corresponds to $|\theta| > \pi/4$.

One of the mass parameters, say m_h^2, can be fixed by requiring the correct electroweak symmetry breaking, $v = 246$ GeV. Then the constraints (27) specify the allowed range of

$$r = \frac{m_s^2}{m_h^2}\ . \tag{32}$$

The required local minimum exists in the following cases:

$$
\begin{aligned}
&\underline{\lambda_{hs} < 0} \\
&\qquad m_h^2 < 0\ ,\ m_s^2 < 0 \quad : \quad 0 < r < \infty\ , \\
&\qquad m_h^2 < 0\ ,\ m_s^2 > 0 \quad : \quad |r| < \frac{|\lambda_{hs}|}{2\lambda_h}\ , \\
&\qquad m_h^2 > 0\ ,\ m_s^2 < 0 \quad : \quad |r| > \frac{2\lambda_s}{|\lambda_{hs}|}\ , \\
&\underline{\lambda_{hs} > 0} \\
&\qquad m_h^2 < 0\ ,\ m_s^2 < 0 \quad : \quad \frac{\lambda_{hs}}{2\lambda_h} < r < \frac{2\lambda_s}{\lambda_{hs}}\ .
\end{aligned}
\tag{33}
$$

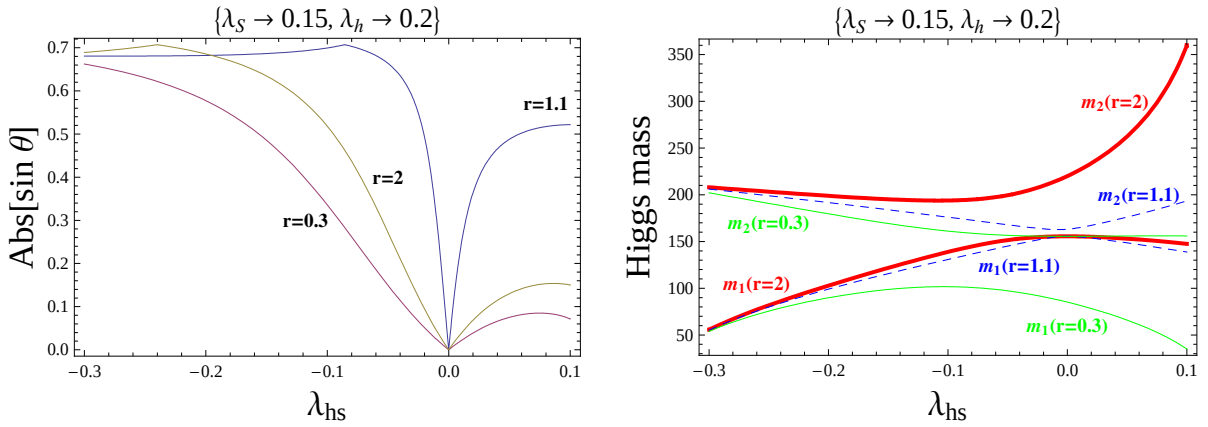


Figure 2: $|\sin\theta|$ and the Higgs masses as functions of λ_{hs} and r for $m_h^2 < 0, m_s^2 < 0$. (Here we redefine θ to be in the range $|\theta| < \pi/4$). The parameter range is consistent with the mixed Higgs–singlet inflaton at $x \sim 1$.

We see that at negative λ_{hs} there is more parameter space available. In fact, negative values of λ_{hs} are preferred by the mixed Higgs-singlet inflaton (Fig. 1), especially away from the point $x = 1$. Indeed, the relations among the couplings ensuring $\langle h\rangle \neq 0, \langle s\rangle \neq 0$ at high and low energies are similar up to $\xi_i \leftrightarrow -m_i^2$. Representative values of the mixing angle consistent with the Higgs-singlet inflaton are displayed in Fig. 2.[3]

Inspection of Eq. (28) shows that the lighter eigenvalue reaches its upper bound at $\lambda_{hs} = 0$. In this case, the mixing angle is zero and

$$
m_1^2 = 2\lambda_h v^2, \tag{34}
$$

[3] Eq. (29) defines θ up to $\pi/2$, so in Fig. 2 we take $|\theta| < \pi/4$. The small kinks in $\sin\theta$ at $\lambda_{hs} = -0.24$ and $\lambda_{hs} = -0.08$ correspond to $|\tan 2\theta| \to \infty$, which signals the change in the nature of the lighter mass eigenstate. In the rest of the paper, we take $-\sin\theta$ to be the h-component of the H_1–state.

as in the Standard Model. According to Fig. 1, this is about 175 GeV. The lower bound on the heavier eigenvalue is also given by Eq. (34). With the lowest allowed λ_h, it is about 135 GeV.

On the other hand, the heavier eigenvalue can be arbitrarily large. Indeed, parametrizing

$$u^2 = v^2 \, \frac{2\lambda_h r - \lambda_{hs}}{2\lambda_s - \lambda_{hs} r} \, , \tag{35}$$

we see that $u \to \infty$ as $r \to 2\lambda_s/\lambda_{hs}$, corresponding to the boundary of the region allowed by (33). In this case, $m_2^2 \simeq 2\lambda_s u^2 \to \infty$ and the mixing angle approaches zero. In terms of the input mass parameters, this corresponds to $|m_{h,s}^2| \to \infty$. The singlet state can also be arbitrarily light: in the limit $r \to \lambda_{hs}/(2\lambda_h)$, u vanishes and the light eigenstate becomes massless.

3.1.1 LEP and electroweak constraints

LEP has set stringent limits on the Higgs mass and couplings. For our purposes, the relevant constraint is given in Fig. 10 of [18], which sets a bound on

$$\zeta^2 \equiv \left(\frac{g_{HZZ}}{g_{HZZ}^{\rm SM}} \right)^2 = |O_{2i}|^2 \tag{36}$$

depending on the mass m_i. For a state with an $\mathcal{O}(1)$ component of h, the bound is

$$m > 114 \text{ GeV} \, , \tag{37}$$

while for a state with a small admixture of h the bound relaxes and can be read off from Fig. 10 of [18]. For example, with $|O_{2i}|^2 \sim 10^{-2}$, the mass can be as low as 20 GeV. In our case, the bound applies to the lighter state only since the mass of the heavier state is greater than $\sqrt{2\lambda_h} v > 114$ GeV. We therefore require that if $m_1 < 114$ GeV, then

$$\sin^2\theta < \zeta^2(m_1) \, . \tag{38}$$

For our purposes, at $\zeta^2 < 0.5$ it suffices to use an approximation $\log_{10}\zeta^2(m) \simeq m/60 - 2.3$ for m measured in GeV, which describes the data within a 95% probability band.

Both mass eigenstates contribute to electroweak observables at a loop level. For example, the correction to the ρ–parameter is [19]

$$\Delta\rho^H = \frac{3G_F}{8\sqrt{2}\pi^2} \sum_i O_{2i}^2 \left(m_W^2 \ln\frac{m_i^2}{m_W^2} - m_Z^2 \ln\frac{m_i^2}{m_W^2} \right) . \tag{39}$$

This is very similar to the SM Higgs contribution and therefore one can easily translate the indirect Higgs mass bounds into a bound on $\sum_i O_{2i}^2 \ln m_i^2$ [19, 20]. As the benchmark numbers

we use the results of [21], $m_H < 148$ GeV (197 GeV) at 95% (99.5%) CL. These bounds also incorporate results of the LEP and Tevatron direct searches, although purely indirect constraints give similar numbers [22]. Keeping in mind that the other oblique as well as vertex corrections behave similar to the ρ–parameter in the heavy Higgs limit and that the sensitivity to the Higgs mass is only logarithmic, we will use the combined fit results to impose

$$\sin^2\theta \ \ln m_1 + \cos^2\theta \ \ln m_2 < \ln 148 \quad (197) \tag{40}$$

at 95% (99.5%) CL, where the masses are measured in GeV.

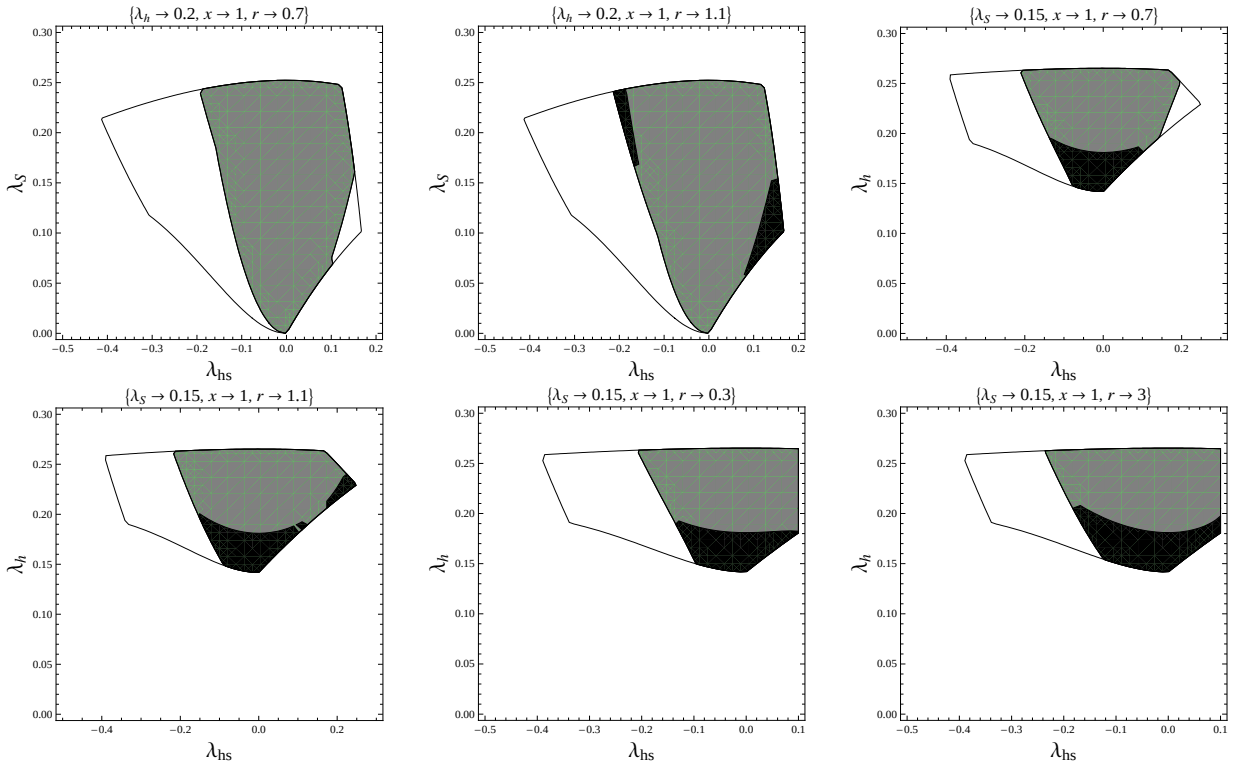


Figure 3: Parameter space allowed by the LEP and electroweak constraints for $m^2_{s,h} < 0$. The region within the contour is allowed by the mixed Higgs-singlet inflaton; grey – allowed by LEP (and automatically consistent with the 99.5% CL electroweak constraints); black – preferred by the 95% CL electroweak constraints. λ_i are given at the scale m_t.

The allowed parameter space is presented in Fig. 3. The main effect of the LEP constraint is to restrict the size of $|\lambda_{hs}|$. The reduction of $|\lambda_{hs}|$ has a two–fold effect: it decreases the mixing angle and (typically) increases the mass of the lighter state (Fig. 2), both of which help satisfy the constraint. As expected, at larger λ_h more parameter space survives. Also, increasing r has a positive effect by making the light state somewhat heavier (Fig. 2).

The 99.5% CL electroweak constraint is satisfied in all the regions allowed by the LEP bound. However, only a relatively small portion of parameter space survives the 95% CL constraint. For instance, none of the points at $\lambda_s = 0.2, r = 0.7$ are allowed. Increasing r to 1.1 opens up some parameter space close to the border of the LEP allowed region. At these points, the nature of the lighter eigenstate changes compared to the $r = 0.7$ case: it becomes Higgs-like. If the light state is singlet-like, it is more difficult to satisfy the EW bound since it is dominated by the term $\cos^2\theta \ \ln m_2$ with $\cos\theta \sim 1$ and $m_2 > \sqrt{2\lambda_h}v$.

In the $\{\lambda_{hs}, \lambda_h\}$ plane, the preferred region is at lower λ_h, typically $\lambda_h < 0.18$. At $r = 0.3$ and $r = 3$, the range of λ_{hs} must be restricted to satisfy (33). As mentioned above, the composition of the lighter state changes with r: it is typically singlet–like at $r < 1$ and Higgs–like otherwise. Thus, at $r = 0.3$ the EW constraint is dominated by $\cos^2\theta \ \ln m_2$, while at $r = 3$ it is dominated by $\sin^2\theta \ \ln m_1$.

A generalization of the analysis to x different from 1 is straightforward. As clear from Fig. 1, at $x \gg 1$ or $x \ll 1$, most points at $\lambda_{hs} > 0$ get eliminated and negative values of λ_{hs} are strongly favored.

The collider signature of the $\langle s\rangle \neq 0$ scenario is a universal suppression of production of the Higgs–like states,

$$\sigma(H_i) = \sigma(h) \ |O_{2i}|^2 \ . \tag{41}$$

It is also possible that the decay $H_2 \to H_1 H_1$ will play a role [23]. It is kinematically allowed when λ_{hs} is considerable (see Fig. 2). Negative λ_{hs} are then largely ruled out by LEP, while positive λ_{hs} are usually consistent with LEP, especially when r is small or large. For example, at $r = 0.3, \lambda_{hs} = 0.05$, the point $m_1 = 57$ GeV, $m_2 = 144$ GeV and $\sin\theta = 0.07$ is allowed by all the constraints. When H_2 is Higgs-like, for $m_2 > 135$ GeV it will decay predominantly into gauge bosons and H_1 pairs. The branching ratio for $H_2 \to H_1 H_1$ scales like $\lambda_{hs}^2 v^4/m_2^4$ [23, 24], which is significant for $\lambda_{hs} > 10^{-1}$ and a light H_2. These values are however disfavored by LEP, so the mode $H_2 \to H_1 H_1$ is only competitive below or close to the WW threshold. In this case, the final state contains 4 b–quarks with relatively low (pairwise) invariant mass. On the other hand, if H_2 is singlet–like, its production cross section is too small and the effect of $H_2 \to H_1 H_1$ is unimportant.

3.2 $\langle h \rangle \neq 0, \langle s \rangle = 0$

In this case,

$$v^2 = -\frac{m_h^2}{\lambda_h} \; . \tag{42}$$

It is a local minimum if

$$\begin{aligned} & m_h^2 < 0 \; , \\ & \lambda_{hs} m_h^2 - 2\lambda_h m_s^2 < 0 \; . \end{aligned} \tag{43}$$

There is no mixing between the Higgs and the singlet, and the mass squared values are

$$m_1^2 = 2\lambda_h v^2 \quad , \quad m_2^2 = \frac{1}{2}\lambda_{hs} v^2 + m_s^2 \; . \tag{44}$$

The allowed range of r is

$$\begin{aligned} & \underline{\lambda_{hs} < 0} \\ & \qquad m_s^2 > 0 \quad : \quad |r| > \frac{|\lambda_{hs}|}{2\lambda_h} \; , \\ & \underline{\lambda_{hs} > 0} \\ & \qquad m_s^2 < 0 \quad : \quad r < \frac{\lambda_{hs}}{2\lambda_h} \; , \\ & \qquad m_s^2 > 0 \quad : \quad 0 < |r| < \infty \; . \end{aligned} \tag{45}$$

The analysis of phenomenological constraints is straightforward. Since $\lambda_h > 0.14$, the Higgs LEP bound is satisfied automatically. The electroweak precision data favor $\lambda_h < 0.18$ (0.32) at 95% (99.5%) CL, as in the Standard Model. The allowed parameter space can then be easily read off from Fig. 1.

A collider signature of the presence of the singlet "hidden sector" would be an invisible decay $h \to ss$, which for $m_1 > 2m_2$ would typically have a significant branching ratio. Note that since $\langle s \rangle = 0$, the symmetry $s \to -s$ is not broken spontaneously and the singlet must be pair–produced. It is relatively easy, especially at small r, to satisfy the kinematic constraint $m_1 > 2m_2$: it requires $\lambda_{hs} < (1 + 2r)\lambda_h$ (see Eq. (44)). The corresponding decay width is [23]

$$\Gamma(h \to ss) = \frac{\lambda_{hs}^2 v^2}{32\pi m_1} \sqrt{1 - \frac{4m_2^2}{m_1^2}} \; . \tag{46}$$

For $\lambda_{hs} \gg 10^{-2}$, this would be the dominant decay mode until the channel $h \to WW$ opens up. Above the WW threshold, its branching ratio drops to $\mathcal{O}(\lambda_{hs}^2 v^4 / m_1^4)$, which can still be significant for $\lambda_{hs} > 10^{-1}$. Note that for the $\langle s \rangle = 0$ case, larger values of $|\lambda_{hs}|$, up to 0.4, are allowed.

3.3 LHC prospects

The Higgs profiling [25] at the LHC depends crucially on whether or not the SM Higgs field mixes with the singlet. If it does, there are two states whose masses can be determined by the resonance peak measurements. The mixing angle can then be determined by the production cross section of these states in a particular production mode. These observables allow us to disentangle 3 quantities (up to a sign ambiguity):

$$m_1, m_2, \sigma_{\rm prod} \Rightarrow \lambda_h v^2, \lambda_s u^2, \lambda_{hs} uv \tag{47}$$

Furthermore, for a sufficiently heavy H_2, measurements of the cascade decay $H_2 \to H_1 H_1$ would determine one more combination of these quantities such that u can be derived [25]. Since v is known from M_W, the couplings λ_h, λ_s and λ_{hs} would then be fixed (the latter up to the sign). In this case, the Lagrangian parameters are (almost fully) reconstructed. Ref. [25] provides an example of a point $\{m_1, m_2, \cos^2\theta\}$=$\{$115 GeV,400 GeV,0.25$\}$, which can be reconstructed with integrated luminosity 300 fb^{-1}. The result is $\lambda_h = 1.04 \pm 0.18$, $u = 55.03 \pm 27.35$ GeV, $\lambda_s = 7.61 \pm 3.51$ and $\lambda_{hs} = 4.52 \pm 2.23$. This example shows that at least in some regions of parameter space, where cascade decays are available, one can determine the low energy Lagrangian. The precision of this reconstruction grows with integrated luminosity. Given the low energy parameters, one can evolve them to high energies and verify whether various inflationary constraints are satisfied. In the example above, the perturbativity constraint is violated. Therefore if such parameter values are indeed found, this would falsify the model.

In the case of small or no mixing, the situation is much more challenging, although the latter option is very interesting as it provides us with a viable dark matter candidate. For a heavy singlet, the only possible signature would be missing energy. If $h \to ss$ is kinematically allowed, the measurement of the Higgs invisible width would determine λ_{hs}, up to a kinematical factor. For Higgs masses above 150 GeV, the invisible decay into dark matter has a small branching fraction and therefore the LHC Higgs exclusion limits apply (see e.g. [26]). For lower Higgs masses, the invisible decay is efficient and λ_{hs} can be determined using the methods of [25]. However, the self–interaction coupling λ_s is unlikely to be measured at the LHC, so the Lagrangian cannot be fully reconstructed in this case.

4 Comparison with the pure singlet or Higgs inflation

It is instructive to compare the above scenario to the pure singlet or Higgs inflation. According to Eq. (12), the singlet inflation ($\tau = 0$) requires at high energies

$$2\lambda_s\xi_h - \lambda_{hs}\xi_s < 0 \,, \tag{48}$$

in which case the "vacuum" energy is $\lambda_s/(4\xi_s^2)$. This immediately implies

$$\lambda_{hs} > 0 \,. \tag{49}$$

The combination $2\lambda_h\xi_s - \lambda_{hs}\xi_h$ can be either positive or negative, depending on whether there exists another local minimum at $\tau = \infty$. We thus leave $2\lambda_h\xi_s - \lambda_{hs}\xi_h$ unconstrained. We further impose the perturbativity and EW vacuum stability bounds (23).[4]

The phenomenological constraints depend crucially whether or not the singlet develops a VEV at low energies. For the case $\langle s\rangle \neq 0$, representative examples are presented in Fig. 4. The existence of the local minimum requires $4\lambda_s\lambda_h - \lambda_{hs}^2 > 0$ at low energies, which together with the LEP Higgs bound eliminates almost all of the parameter space at $x = \xi_s/\xi_h \sim 1$. For $\lambda_s = 0.15$ and $x = 1.5$, Eq. (48) requires $\lambda_{hs} > 0.2$ at μ_U. Due to the positive RG contribution from λ_h, this bound is easier to satisfy at larger λ_h, hence the slanted boundary on the left. Perturbativity and stability further cut off large values of λ_h, λ_{hs} and small values of λ_h.

Considerable parameter space is only available at $x \gg 1$, in which case (48) amounts to positivity of λ_{hs} and the allowed region is mainly constrained by the perturbativity and stability considerations. Since λ_{hs} contributes positively to the running of λ_h, smaller values of the latter are allowed by $\lambda_h(\mu_U) > 0$ at large λ_{hs}. On the other hand, λ_{hs} beyond 0.2 is ruled out by the LEP bound. The 99.5% CL electroweak precision constraint is satisfied in the entire region, while the 95% CL limit prefers λ_h at the lower end.

If the singlet has a zero VEV, there is no Higgs–singlet mixing and the low energy constraints relax. The analysis is very similar to that of Sec. 3.2 and phenomenology restricts the values of λ_h within the inflation–allowed contours of Fig. 4. For example, the EW preferred region is $\lambda_h < 0.18$.

Finally, Higgs inflation ($\tau = \infty$) requires

$$2\lambda_h\xi_s - \lambda_{hs}\xi_h < 0 \tag{50}$$

[4]Note that singlet inflation is impossible for negative λ_{hs} even if $\xi_s \gg \xi_h$. In this case, the point $h = 0, s \to \infty$ is unstable and h rolls to infinity. Similarly, Higgs inflation is impossible for $\lambda_{hs} < 0$. For positive λ_{hs}, our numerical results are in qualitative agreement with those of [7, 8].

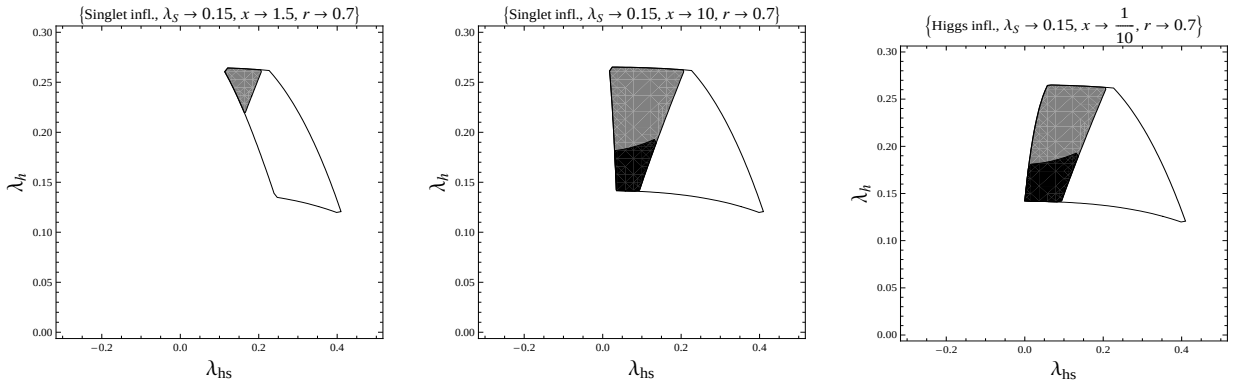


Figure 4: Constraints on pure singlet and Higgs inflation. The region within the contour is consistent with singlet (left, center) and Higgs (right) inflation; grey – allowed by $\langle s\rangle \neq 0$ and LEP; black – favored by the 95% CL electroweak constraints. Here $m^2_{s,h} < 0$ and λ_i are given at the scale m_t.

at high energies, which again implies $\lambda_{hs} > 0$. Significant parameter space exists only at $x \ll 1$ and the above considerations largely apply, up to $h \leftrightarrow s$. An example is shown in the right panel of Fig. 4.

The main difference between the "mixed" and "pure" inflaton scenarios lies in the sign of λ_{hs}: the former allows for both signs, while the latter requires a positive λ_{hs}. Note that $\lambda_{hs} > 0$ typically leads to $\langle s\rangle = 0$ for a wide range of the parameters, while $\lambda_{hs} < 0$ prefers $\langle s\rangle \neq 0$ (see Eqs. (33),(45)). Thus the "pure" inflation would favor no singlet–Higgs mixing at low energies and the only collider signature of the singlet would be an invisible decay $h \to ss$, if kinematically allowed. In the mixed inflaton case, $\langle s\rangle = 0$ and $\langle s\rangle \neq 0$ are almost equally likely. One therefore often expects Higgs–singlet mixing at low energies which would manifest itself in the existence of 2 Higgs–like states with universally suppressed couplings to the SM fields.

We also observe that, at $\lambda_{hs} > 0$, there is an overlap in the allowed parameter space for the mixed and pure inflaton (at different x), so the collider data alone may not be sufficient to discriminate among the different scenarios.[5]

5 Unitarity issues

The most problematic aspect of Higgs inflation and alike has to do with unitarity. In the presence of large non-minimal couplings to gravity, unitarity violation appears around the inflation

[5]Presently it also seems challenging to determine the sign of λ_{hs} at the LHC. One is likely to need a linear collider to measure scalar self–interactions.

(Hubble) scale $M_{\rm Pl}/\xi$ [4, 5]. This signals that the theory as it stands is incomplete and should be supplemented by additional fields [6] or operators [27] at high energies.

To see how unitarity violation comes about, consider our setup at field values $|h| \ll 1/\xi_h$ and $|s| \ll 1/\xi_s$ in Planck units. With Ω^2 given in Eq. (4), the kinetic terms are

$$\mathcal{L}_{\rm kin} = \frac{3}{4}\Big(\partial_\mu \log(1+\xi_h h^2+\xi_s s^2)\Big)^2 + \frac{1}{2}\frac{1}{1+\xi_h h^2+\xi_s s^2}\Big((\partial_\mu h)^2+(\partial_\mu s)^2\Big)\,. \tag{51}$$

To leading order in $h\xi_h$ and $s\xi_s$, the mixing between h and s is negligible and we have

$$\mathcal{L}_{\rm kin} \simeq \frac{1}{2}(1+6\xi_s^2 s^2)(\partial_\mu s)^2 + \frac{1}{2}(1+6\xi_h^2 h^2)(\partial_\mu h)^2\,. \tag{52}$$

The canonically normalized variables are therefore

$$\rho = s(1+\xi_s^2 s^2), \quad \varphi = h(1+\xi_h^2 h^2)\,. \tag{53}$$

We can now expand the fields in terms of expectation values and fluctuations:

$$\rho = \rho_0 + \bar\rho\,,\ \varphi = \varphi_0 + \bar\varphi\,, \tag{54}$$

and, similarly, $s = s_0 + \bar s$ and $h = h_0 + \bar h$. The fluctuations of the original and the canonically normalized fields are related by $\bar s \simeq (1-3\xi_s^2 s_0^2)\bar\rho - 3\xi_s^2 s_0\,\bar\rho^2$ and $\bar h \simeq (1-3\xi_h^2 h_0^2)\bar\varphi - 3\xi_h^2 h_0\,\bar\varphi^2$.

Consider interactions of the Higgs with the gauge bosons. The conformal rescaling brings in terms of order $\xi_h h^2$ and $\xi_s s^2$, which are negligible compared to $\xi_h^2 h^2$ and $\xi_s^2 s^2$. We thus have

$$\mathcal{L}_{\rm gauge} = \frac{1}{2}g^2 h^2 W_\mu^+ W^{\mu-} \tag{55}$$

$$= \frac{1}{2}g^2\varphi_0^2\Big(1+2a\frac{\bar\varphi}{\varphi_0}+b\frac{\bar\varphi^2}{\varphi_0^2}\Big)W_\mu^+ W^{\mu-} \tag{56}$$

with $a = 1-3\xi_h^2\varphi_0^2$ and $b = 1-12\xi_h^2\varphi_0^2$. Here we have neglected the difference between φ_0 and h_0. We see that the Standard Model gauge–Higgs interactions ($a = b = 1$) have changed due to the non–canonical normalization. It means that the Higgs exchange no longer unitarizes the WW scattering and the amplitude grows with energy: $\mathcal{A}(WW\to WW) \sim E^2\Delta a/\varphi_0^2 \sim \xi_h^2 E^2$, where Δa is the deviation of a from its SM value. Thus unitarity is violated at $E \sim 1/\xi_h$.

Furthermore, unitarity is violated by scalar interactions. Rewriting the Einstein frame scalar potential in terms of φ and ρ, we get

$$U \simeq \frac{1}{4}\lambda_h\varphi^4(1-4\xi_h^2\varphi^2) + \frac{1}{4}\lambda_s\rho^4(1-4\xi_s^2\rho^2) + \frac{1}{4}\lambda_{hs}\varphi^2\rho^2(1-2\xi_h^2\varphi^2-2\xi_s^2\rho^2)\,. \tag{57}$$

The 6–point interactions induce $2\to 4$ scattering with a cross section growing as E^2/Λ^4 with $\Lambda = 1/\xi_{s,h}$, while the unitary bound is $1/E^2$. Again, for $E > 1/\xi_{s,h}$, unitarity is violated.

5.1 Example of unitarization

We see that at the scale $1/\xi_{s,h}$ new physics unitarizing scattering amplitudes should show up. It may come in a form of new degrees of freedom and/or new operators. One possibility is to complete the theory into a σ–model by adding a heavy scalar σ [6]. The corresponding Jordan–frame Lagrangian reads

$$\begin{aligned}\mathcal{L}_J/\sqrt{-g_J} &= -\frac{1}{2}(\xi_\sigma\sigma^2+\tilde{\xi}_h h^2+\tilde{\xi}_s s^2)R+\frac{1}{2}(\partial_\mu\sigma)^2+\frac{1}{2}(\partial_\mu h)^2+\frac{1}{2}(\partial_\mu s)^2 \\ &\quad -\frac{1}{4}\kappa(\sigma^2-\Lambda^2-\alpha h^2-\beta s^2)^2-V_J(h,s)\ , \end{aligned} \tag{58}$$

where $V_J(h,s)$ is the Higgs portal potential and $\Lambda=1/\sqrt{\xi_\sigma}$. Here the VEV of σ generates the Planck scale (one may also add a bare M^2R term [6]) and we take $\tilde{\xi}_h,\tilde{\xi}_s \ll \xi_\sigma$; $\Lambda \gg v,u$. In the low energy limit, the heavy σ–field can be integrated out by minimizing the scalar potential (in the Jordan or Einstein frames),

$$\sigma^2=\Lambda^2+\alpha h^2+\beta s^2\ . \tag{59}$$

The resulting effective action is that of the Higgs portal inflation with effective couplings to gravity $\xi_h=\tilde{\xi}_h+\alpha\xi_\sigma\simeq\alpha\xi_\sigma$ and $\xi_s=\tilde{\xi}_s+\beta\xi_\sigma\simeq\beta\xi_\sigma$.

One can easily verify that in the vacuum (at small u,v) the canonically normalized field in the Einstein frame is $\chi=\sqrt{6}\ln(\sigma/\Lambda)$ with mass of order $\sqrt{\kappa}/\xi_\sigma$. Substituting $\sigma=\Lambda\exp(\chi/\sqrt{6})$ back in the potential, one finds that the non-renormalizable interactions of χ are Planck–suppressed. On the other hand, since $\tilde{\xi}_{h,s}\sim\mathcal{O}(1)$, unitarity constraints for interactions of h and s are satisfied up to the Planck scale energies.

Let us now consider the inflationary regime $\sigma\gg\Lambda$. The kinetic terms in the Einstein frame are given by

$$\begin{aligned}\mathcal{L}_{\rm kin} &= \frac{3}{4}\Big[\partial_\mu\ln(\xi_\sigma\sigma^2+\tilde{\xi}_h h^2+\tilde{\xi}_s s^2)\Big]^2 \\ &\quad +\frac{1}{2(\xi_\sigma\sigma^2+\tilde{\xi}_h h^2+\tilde{\xi}_s s^2)}\cdot\Big[(\partial_\mu\sigma)^2+(\partial_\mu h)^2+(\partial_\mu s)^2\Big]\ . \end{aligned} \tag{60}$$

Defining

$$\chi=\sqrt{\frac{3}{2}}\ln(\xi_\sigma\sigma^2)\ ,\ \tau_h=\frac{h}{\sigma}\ ,\ \tau_s=\frac{s}{\sigma}\ , \tag{61}$$

we find to leading order in $1/\xi_\sigma$,

$$\mathcal{L}_{\rm kin}=\frac{1}{2}(\partial_\mu\chi)^2+\frac{1}{2\xi_\sigma}(\partial_\mu\tau_h)^2+\frac{1}{2\xi_\sigma}(\partial_\mu\tau_s)^2\ , \tag{62}$$

while the mixing terms are further suppressed. The Einstein frame scalar potential is

$$U = (\xi_\sigma \sigma^2 + \tilde{\xi}_h h^2 + \tilde{\xi}_s s^2)^{-2} \left[\frac{1}{4} \kappa (\sigma^2 - \Lambda^2 - \alpha h^2 - \beta s^2)^2 + V_J(h,s) \right] , \tag{63}$$

which at large σ and ξ_σ becomes

$$U \simeq \frac{1}{4\xi_\sigma^2} \left[\kappa (1 - \alpha \tau_h^2 - \beta \tau_s^2)^2 + \lambda_h \tau_h^4 + \lambda_s \tau_s^4 + \lambda_{hs} \tau_h^2 \tau_s^2 \right] . \tag{64}$$

The extremum at $\tau_{h,s} \neq 0$ ("mixed inflaton") is given by

$$\begin{aligned} \tau_h^2 &= \frac{2\kappa(2\alpha\lambda_s - \beta\lambda_{hs})}{4\lambda_h\lambda_s - \lambda_{hs}^2 + 4\kappa(\alpha^2\lambda_h + \beta^2\lambda_s - \alpha\beta\lambda_{hs})}, \\ \tau_s^2 &= \frac{2\kappa(2\beta\lambda_h - \alpha\lambda_{hs})}{4\lambda_h\lambda_s - \lambda_{hs}^2 + 4\kappa(\alpha^2\lambda_h + \beta^2\lambda_s - \alpha\beta\lambda_{hs})} . \end{aligned} \tag{65}$$

It is a local minimum if

$$\begin{aligned} & 2\alpha\lambda_s - \beta\lambda_{hs} > 0, \\ & 2\beta\lambda_h - \alpha\lambda_{hs} > 0, \\ & 4\lambda_h\lambda_s - \lambda_{hs}^2 + 4\kappa(\alpha^2\lambda_h + \beta^2\lambda_s - \alpha\beta\lambda_{hs}) > 0 . \end{aligned} \tag{66}$$

The last condition follows from the positivity of the determinant of the Hessian. The value of the potential at this point determines the energy density during inflation with heavy $\tau_{h,s}$ integrated out. The resulting inflaton potential is

$$U(\chi) = \frac{\lambda_{\rm eff}}{4\xi_\sigma^2} \left(1 + \exp\left(-\frac{2\chi}{\sqrt{6}} \right) \right)^{-2} \tag{67}$$

with

$$\lambda_{\rm eff} = \kappa \, \frac{4\lambda_h\lambda_s - \lambda_{hs}^2}{4\lambda_h\lambda_s - \lambda_{hs}^2 + 4\kappa(\alpha^2\lambda_s + \beta^2\lambda_s - \alpha\beta\lambda_{hs})} . \tag{68}$$

The denominator of $\lambda_{\rm eff}$ is positive by the stability condition (66), so positivity of the energy density during inflation requires $4\lambda_h\lambda_s - \lambda_{hs}^2 > 0$. Recalling that $\xi_h \simeq \alpha\xi_\sigma$ and $\xi_s \simeq \beta\xi_\sigma$, this condition together with (66) implies

$$\begin{aligned} & 2\lambda_h\xi_s - \lambda_{hs}\xi_h > 0 , \\ & 2\lambda_s\xi_h - \lambda_{hs}\xi_s > 0 , \\ & 4\lambda_s\lambda_h - \lambda_{hs}^2 > 0 . \end{aligned} \tag{69}$$

These are exactly the conditions we imposed in our parameter space analysis, Eq. (22).[6] Note also that inflation proceeds at the same $\tau = \tau_h/\tau_s$ as in the original model.

[6] Note also that $\alpha^2\lambda_h + \beta^2\lambda_s - \alpha\beta\lambda_{hs} > 0$ follows from $2\alpha\lambda_s - \beta\lambda_{hs} > 0, 2\beta\lambda_h - \alpha\lambda_{hs} > 0$ (for positive α, β).

Therefore, unitarized Higgs portal inflation leads to the same constraints on the couplings as the original model does. This is despite the fact that now all three fields participate in inflation, $\tau_{h,s} = \mathcal{O}(1)$, and the theory involves an unknown couplings κ. The latter affects the energy density, but not the shape of the potential, so the predictions for the inflationary parameters $n \simeq 0.97$ and $r \simeq 0.0033$ hold.

6 Conclusion

We have studied an extension of the Higgs sector with a real scalar in the presence of large couplings to scalar curvature. This system supports inflation at large field values, with tree level predictions $n \simeq 0.97$ and $r \simeq 0.0033$.

The nature of the inflaton depends on the relations among the couplings. For instance, at negative λ_{hs}, the inflaton is a mixture of the Higgs and the singlet, while at positive λ_{hs} it can also be a pure Higgs or a singlet. These requirements leave an imprint on the low energy phenomenology, e.g. the "mixed" inflation often leads to mixed Higgs–singlet mass eigenstates at low energies. The latter would manifest themselves at the LHC as 2 Higgs–like states with universally suppressed couplings.

We have shown how Higgs portal inflation can be unitarized by adding an extra scalar with a sub–Planckian VEV. This extension does not however affect the constraints on the couplings and the low energy phenomenology remains the same.

Acknowledgements. HML is supported by a CERN–Korean fellowship.

References

[1] A. H. Guth, Phys. Rev. D **23**, 347 (1981); A. D. Linde, Phys. Lett. B **108**, 389 (1982); A. Albrecht and P. J. Steinhardt, Phys. Rev. Lett. **48**, 1220 (1982).

[2] F. L. Bezrukov and M. Shaposhnikov, Phys. Lett. B **659**, 703 (2008); F. Bezrukov, A. Magnin, M. Shaposhnikov and S. Sibiryakov, JHEP **1101** (2011) 016.

[3] B. Patt and F. Wilczek, arXiv:hep-ph/0605188.

[4] C. P. Burgess, H. M. Lee and M. Trott, JHEP **0909** (2009) 103; J. L. F. Barbon and J. R. Espinosa, Phys. Rev. D **79** (2009) 081302 (2009) 081302; M. P. Hertzberg, JHEP **1011**, 023 (2010).

[5] C. P. Burgess, H. M. Lee and M. Trott, JHEP **1007** (2010) 007.

[6] G. F. Giudice and H. M. Lee, Phys. Lett. B **694** (2011) 294.

[7] T. E. Clark, B. Liu, S. T. Love and T. ter Veldhuis, Phys. Rev. D **80** (2009) 075019.

[8] R. N. Lerner and J. McDonald, Phys. Rev. D **80** (2009) 123507.

[9] N. Okada and Q. Shafi, arXiv:1007.1672 [hep-ph]; R. N. Lerner and J. McDonald, arXiv:1104.2468 [hep-ph].

[10] D. S. Salopek, J. R. Bond and J. M. Bardeen, Phys. Rev. D **40**, 1753 (1989).

[11] D. H. Lyth and A. Riotto, Phys. Rept. **314**, 1 (1999).

[12] J. O. Gong and H. M. Lee, arXiv:1105.0073.

[13] F. L. Bezrukov, A. Magnin and M. Shaposhnikov, Phys. Lett. B **675**, 88 (2009).

[14] A. De Simone, M. P. Hertzberg and F. Wilczek, Phys. Lett. B **678**, 1 (2009).

[15] A. O. Barvinsky, A. Y. Kamenshchik and A. A. Starobinsky, JCAP **0811**, 021 (2008); A. O. Barvinsky, A. Y. Kamenshchik, C. Kiefer, A. A. Starobinsky and C. Steinwachs, JCAP **0912**, 003 (2009).

[16] F. Bezrukov, M. Shaposhnikov, JHEP **0907**, 089 (2009).

[17] U. Langenfeld, S. O. Moch and P. Uwer, arXiv:1006.0097.

[18] R. Barate *et al.* [LEP Working Group for Higgs boson searches and ALEPH Collaboration and and], Phys. Lett. B **565**, 61 (2003).

[19] D. G. Cerdeno, A. Dedes and T. E. J. Underwood, JHEP **0609**, 067 (2006).

[20] J. D. Wells, arXiv:0803.1243.

[21] J. Erler, Phys. Rev. D **81**, 051301 (2010).

[22] K. Nakamura *et al.* [Particle Data Group], J. Phys. G **37**, 075021 (2010); H. Flacher, M. Goebel, J. Haller, A. Hocker, K. Monig and J. Stelzer, Eur. Phys. J. C **60**, 543 (2009).

[23] M. Bowen, Y. Cui and J. D. Wells, JHEP **0703**, 036 (2007).

[24] A. Djouadi, Phys. Rept. **457**, 1 (2008).

[25] C. Englert, T. Plehn, D. Zerwas, P. M. Zerwas, Phys. Lett. **B703**, 298-305 (2011).

[26] I. Low, P. Schwaller, G. Shaughnessy, C. E. M. Wagner, [arXiv:1110.4405 [hep-ph]].

[27] R. N. Lerner and J. McDonald, Phys. Rev. D **82** (2010) 103525.